

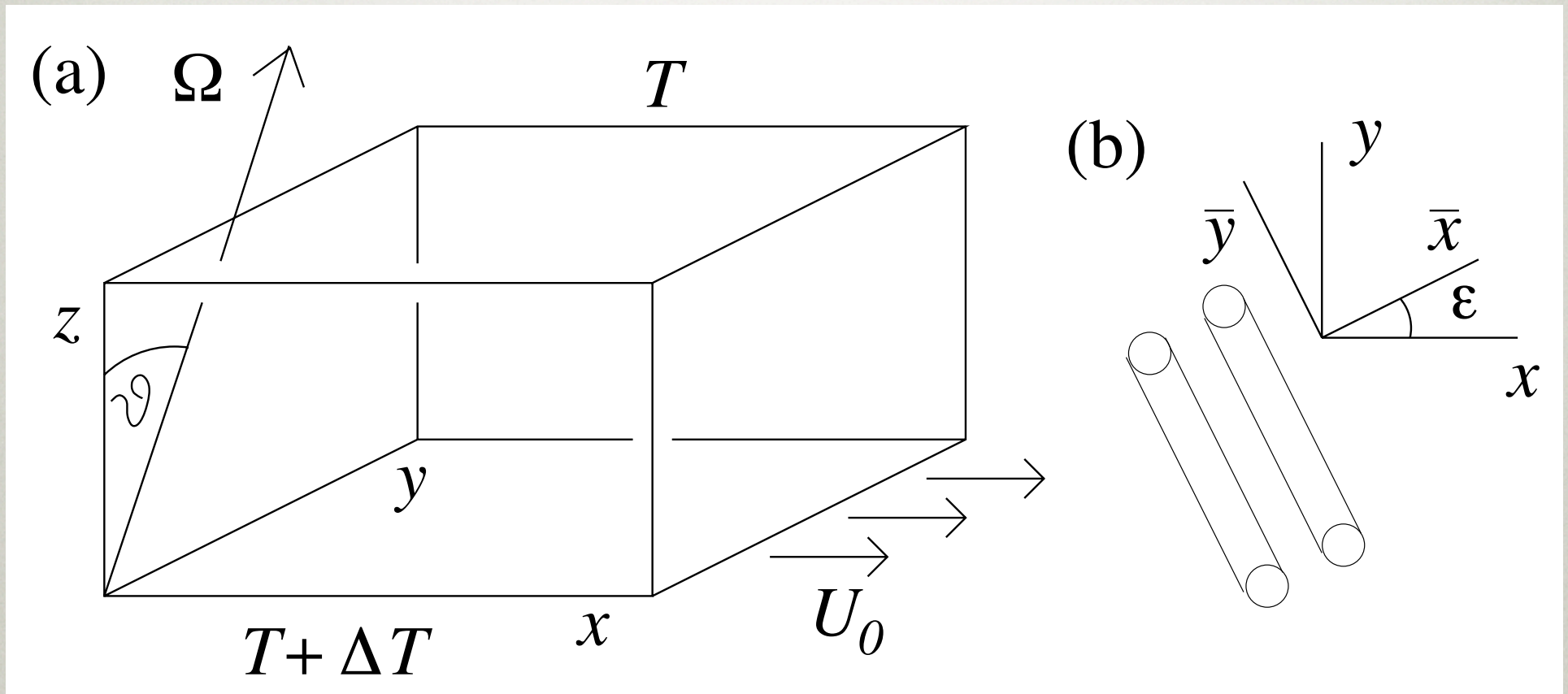
# NONLINEAR DYNAMOS DRIVEN BY SHEAR FLOWS

PU ZHANG, ANDREW GILBERT,  
ANDREW SOWARD, KEKE ZHANG,  
YANNICK PONTY.

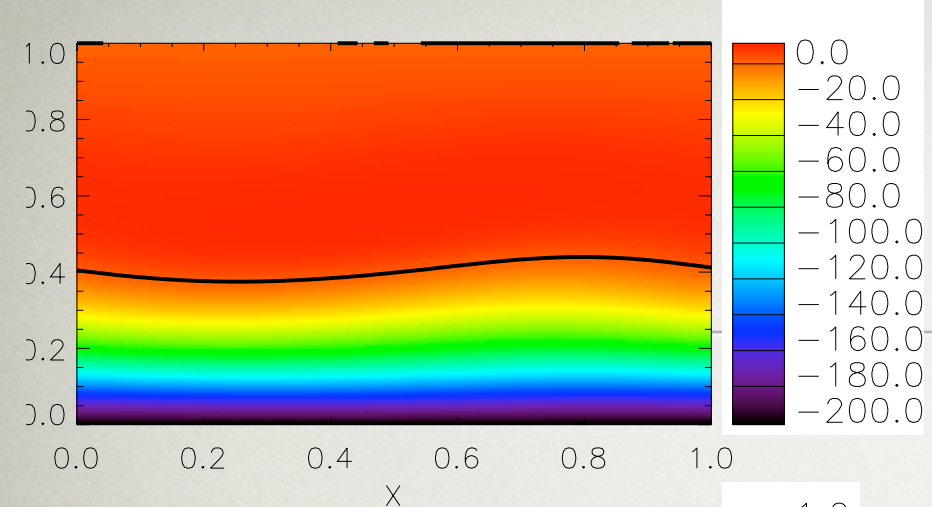
WITH THANKS TO THE LEVERHULME TRUST.

St Andrew's  
UK-MHD-06

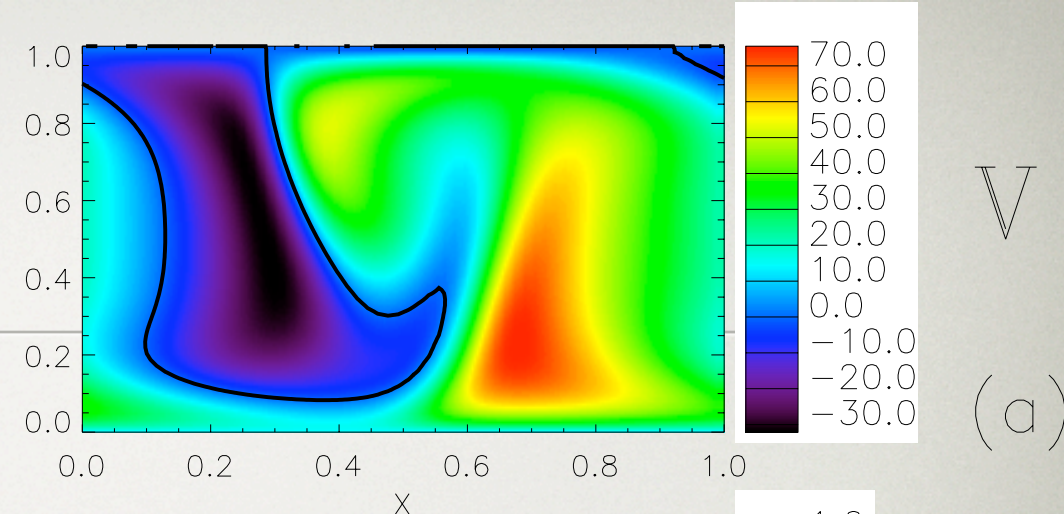
# GEOMETRY: FLOWS DRIVEN BY SHEAR AND/OR CONVECTION



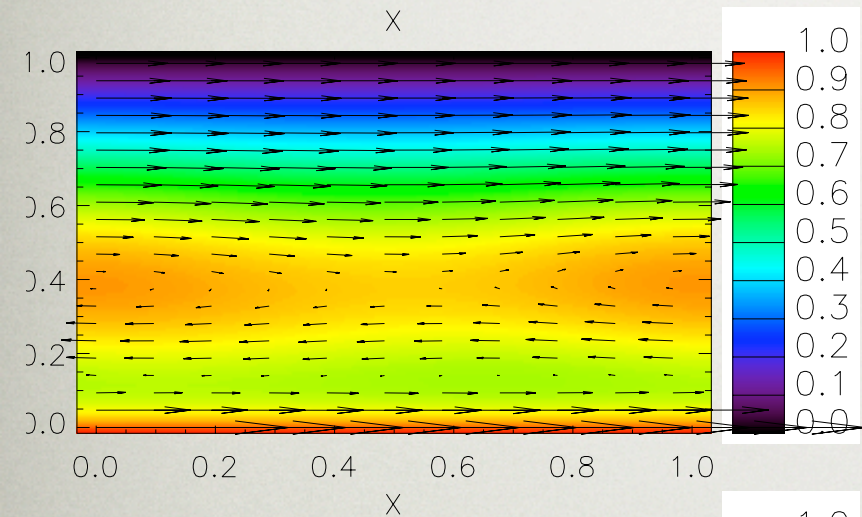
Flow driven by shear or convection in a rotating frame. Ekman layer can become unstable giving cat's eye rolls (Ponty, Gilbert, Soward 2001).



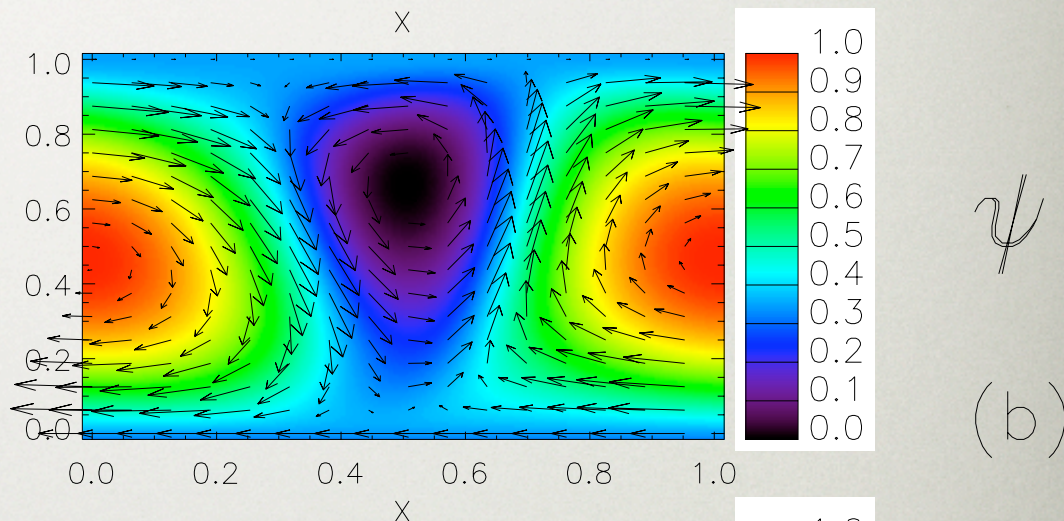
$V$   
(a)



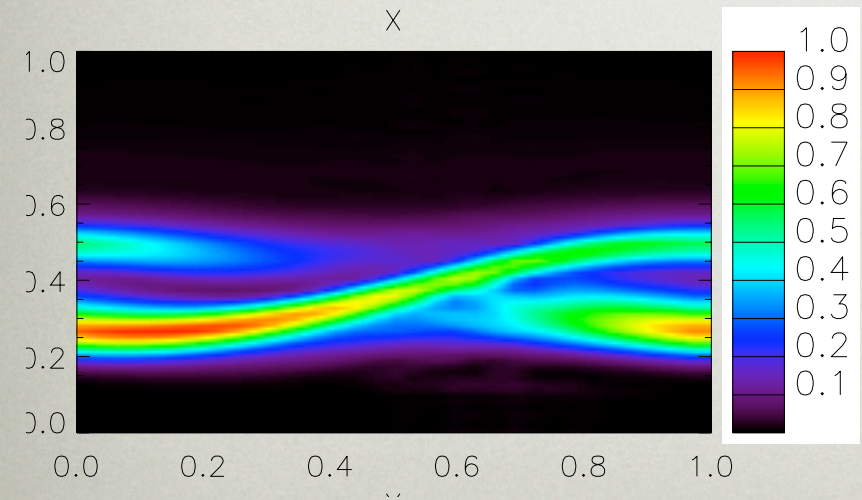
$V$   
(a)



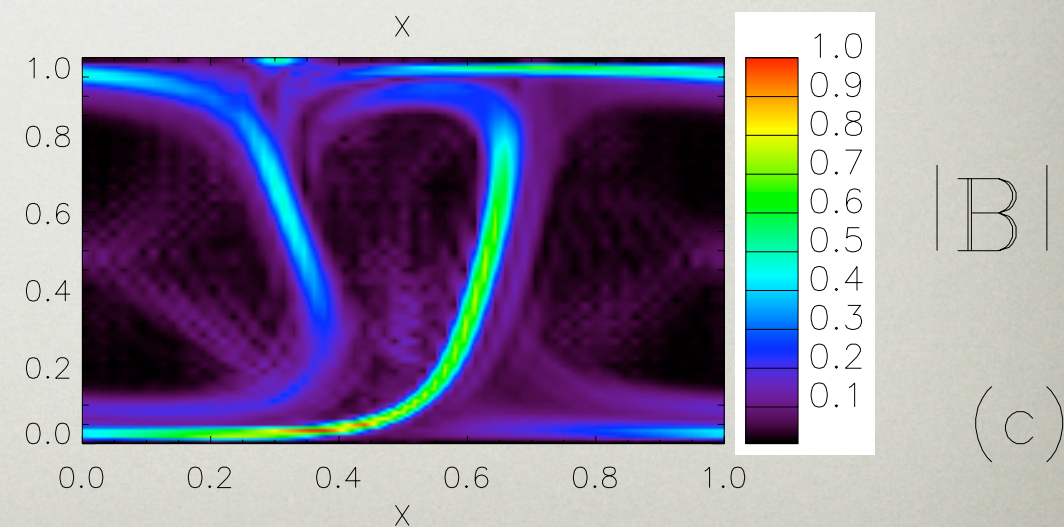
$\psi$   
(b)



$\psi$   
(b)



$|B|$   
(c)



$|B|$   
(c)

Ekman instability

Convective instability

# EQUATIONS AND

**PARAMETERS:**  $\{\text{Re}, \tau, \text{Pm}, \vartheta, \varepsilon, k_{\bar{x}}, k_{\bar{y}}\}$ . •

---

$$\frac{\partial \mathbf{U}}{\partial t} + \mathbf{U} \cdot \nabla \mathbf{U} + \tau \hat{\boldsymbol{\Omega}} \times \mathbf{U} = -\nabla \Pi + (\nabla \times \mathbf{B}) \times \mathbf{B} + \nabla^2 \mathbf{U},$$

$$\frac{\partial \mathbf{B}}{\partial t} = \nabla \times (\mathbf{U} \times \mathbf{B}) + \text{Pm}^{-1} \nabla^2 \mathbf{B},$$

$$\nabla \cdot \mathbf{U} = 0, \quad \nabla \cdot \mathbf{B} = 0$$

$$\vartheta, \quad \text{Re} = \frac{U_0 h}{\nu}, \quad \tau = \frac{2\Omega h^2}{\nu}, \quad \text{Pm} = \frac{\nu}{\eta},$$

The Magnetic Reynolds number becomes a diagnostic defined by:

$$\text{Rm} = \text{Pm} U, \quad U \equiv \sqrt{2E_K}, \quad E_K = \frac{1}{2} \langle \mathbf{U}^2 \rangle$$

# KINETIC ENERGY & DYNAMO GROWTH RATES

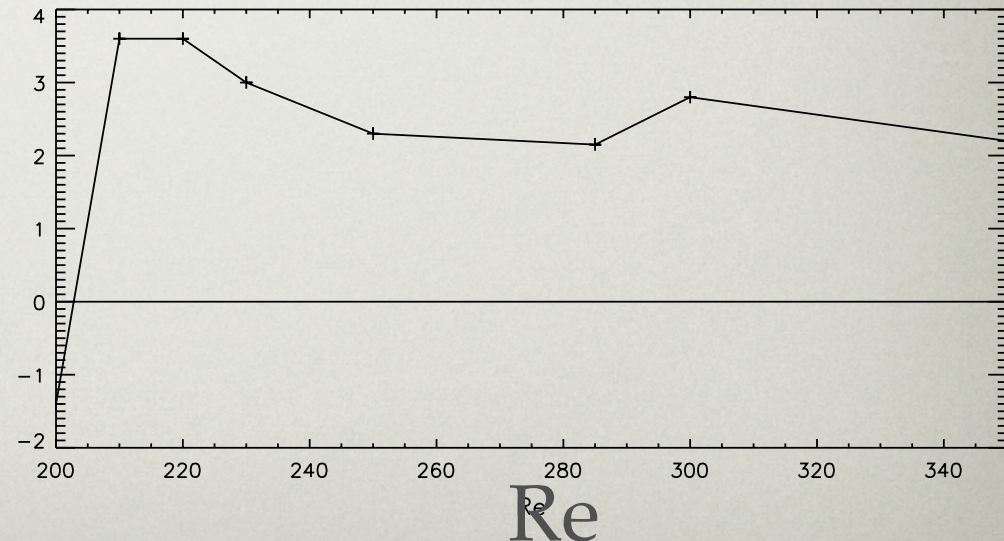
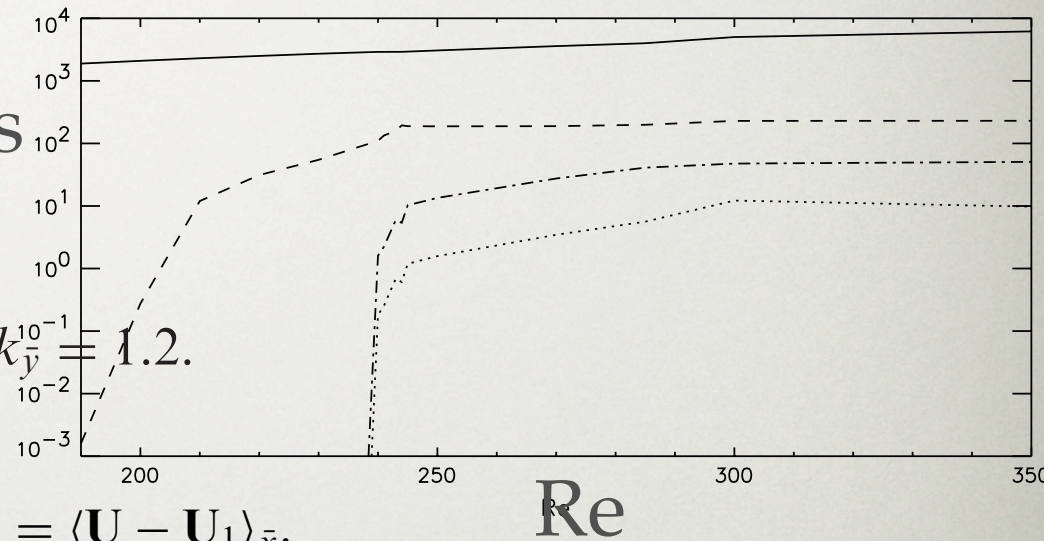
Energy in different components  
of Ekman flow for:

$$\tau = 60, \quad \vartheta = 45^\circ, \quad \varepsilon = 73.5^\circ, \quad k_{\bar{x}} = 3.44, \quad k_{\bar{y}}^{10^{-1}} = 1.2.$$

$$E_K = E_{K1} + E_{K2\bar{x}} + E_{K2\bar{y}} + E_{K3}$$

$$U_1(z) = \langle \mathbf{U} \rangle_{\bar{x}, \bar{y}}, \quad U_{2\bar{x}}(\bar{x}, z) = \langle \mathbf{U} - \mathbf{U}_1 \rangle_{\bar{y}}, \quad U_{2\bar{y}}(\bar{y}, z) = \langle \mathbf{U} - \mathbf{U}_1 \rangle_{\bar{x}}.$$

Kinematic dynamo  
growth rates at:  
 $Pm = 50.$



$$U_z(\bar{x}, \bar{y}, \frac{1}{2}) \text{ (left), } \bar{B}(\bar{x}, z) \equiv \sqrt{\langle |\mathbf{B}|^2 \rangle_{\bar{y}}} \text{ (middle), } \bar{B}_{\bar{x}}(\bar{y}, z) \equiv \langle B_{\bar{x}} \rangle_{\bar{x}} \text{ (right).}$$

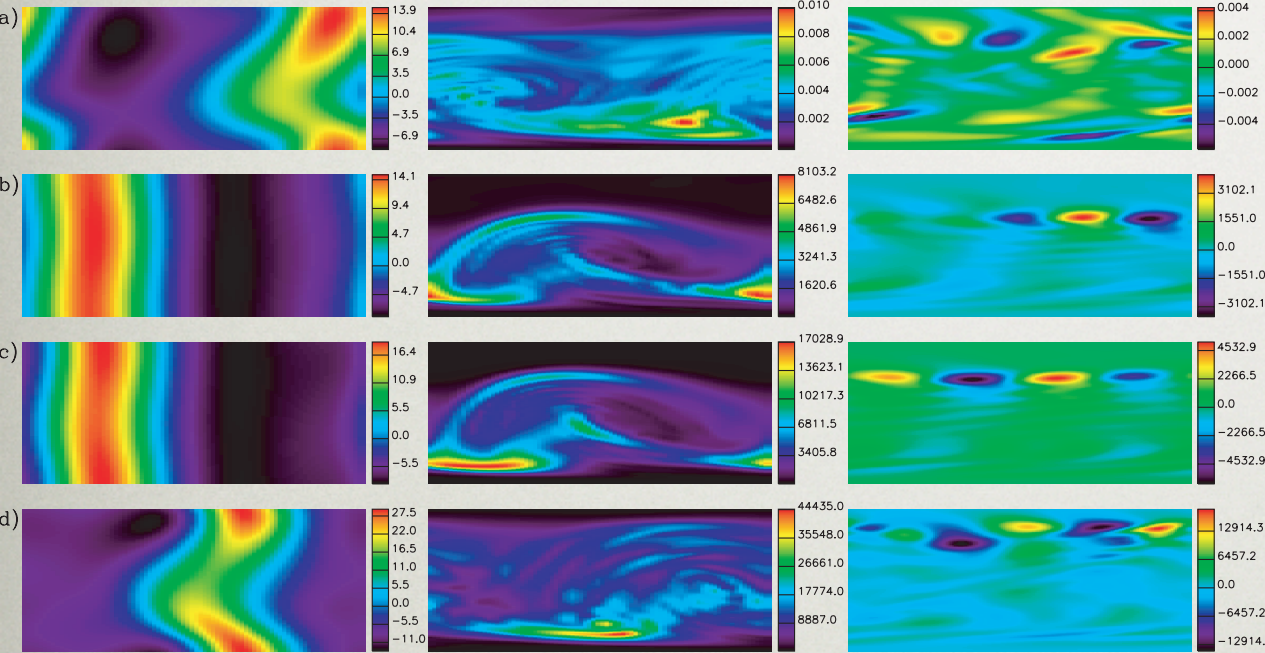
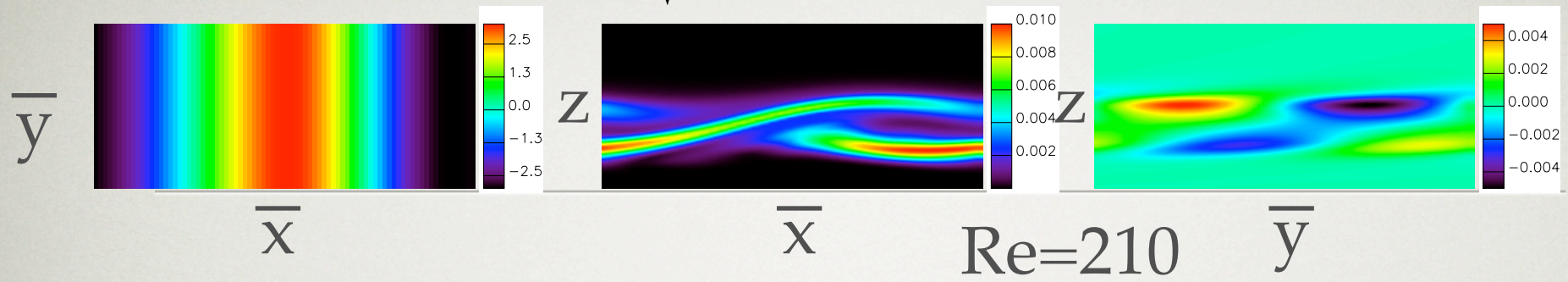


Figure 6. Snapshots of flow and magnetic field diagnostics (21) as in figure 3, in the kinematic regime at times (a)  $t=21.5$ , (b)  $t=22$ , (c)  $t=22.2$ , and (d)  $t=22.4$ .

Re=250

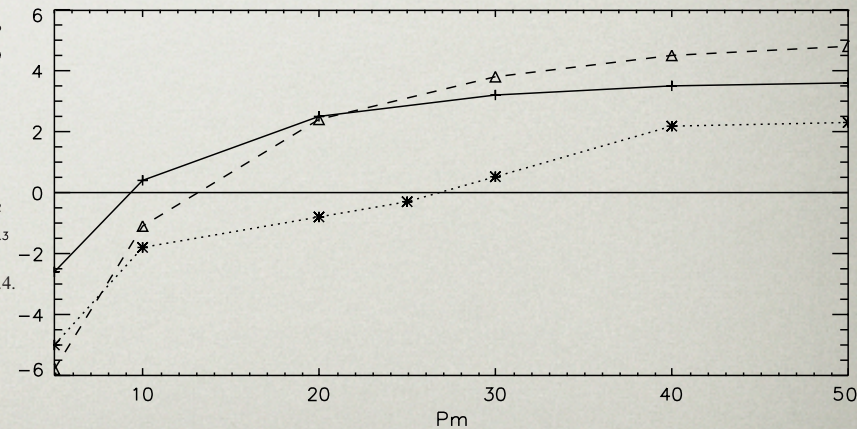
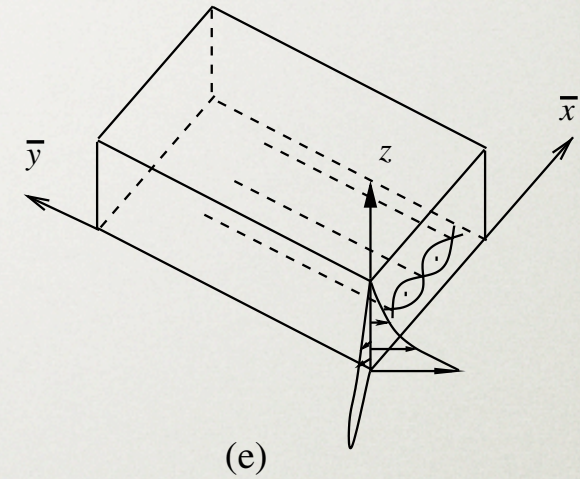
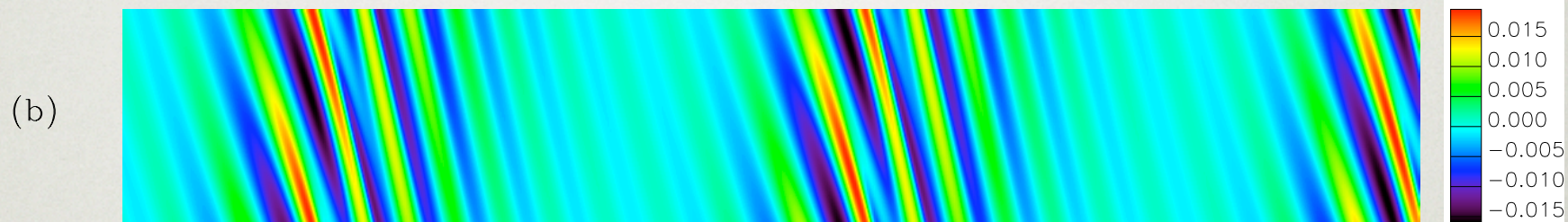
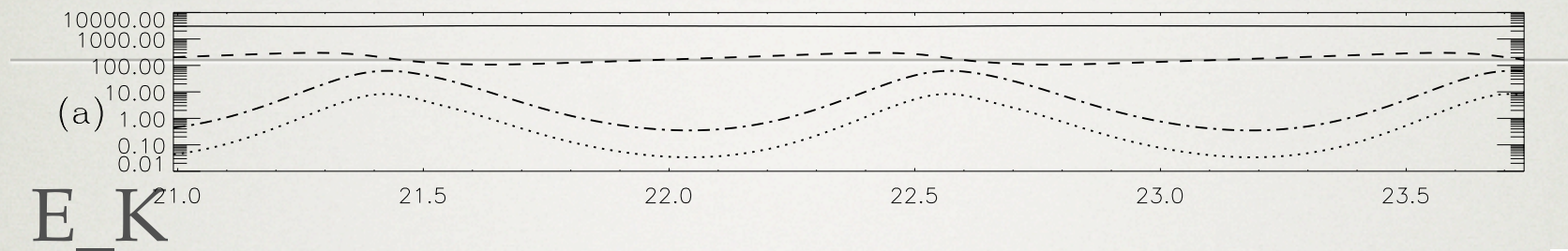
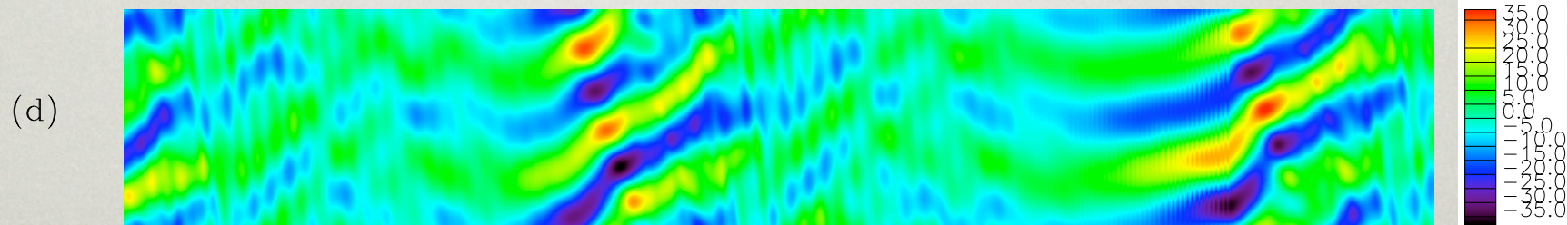
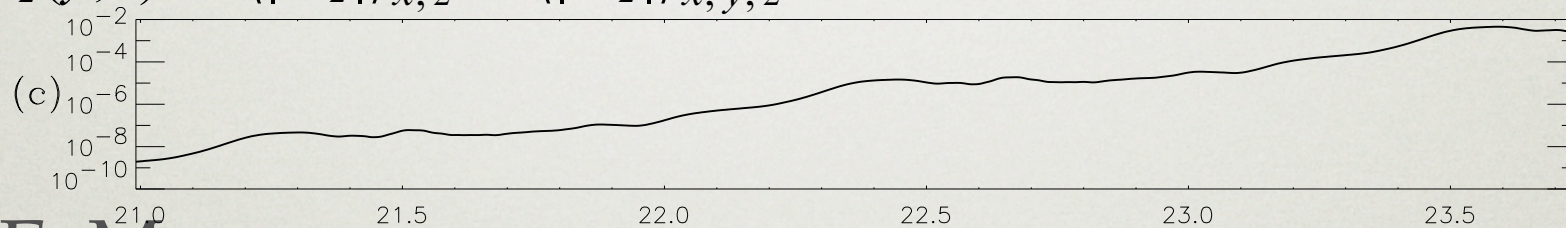


Figure 4. Magnetic growth rate  $\sigma$  as a function of  $Pm$  for the Ekman layer flow with parameters (21) and  $Re=210$  (solid),  $Re=250$  (dotted). The dashed curve gives growth rates for the Taylor-Couette flow with parameters (24).

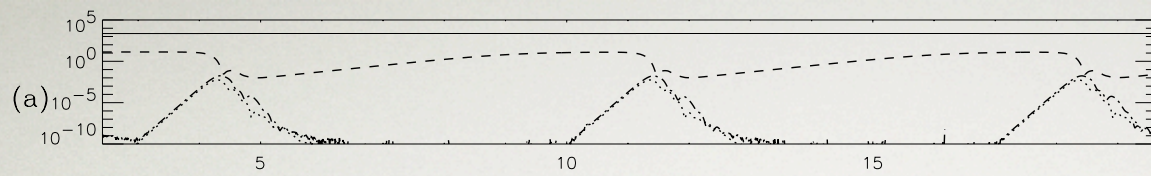
# KINEMATIC BEHAVIOUR



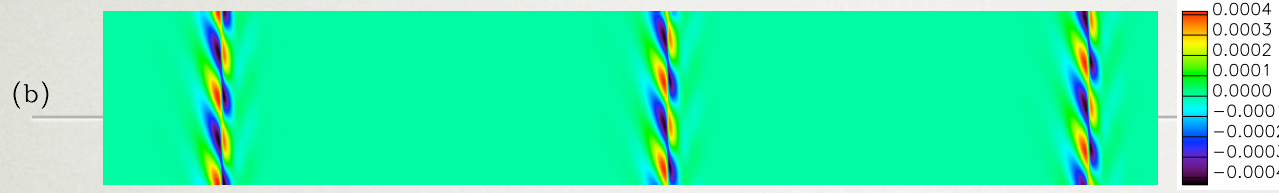
$$\hat{U}_z(\bar{y}, t) = \langle |U_z| \rangle_{\bar{x}, z} - \langle |U_z| \rangle_{\bar{x}, \bar{y}, z}$$



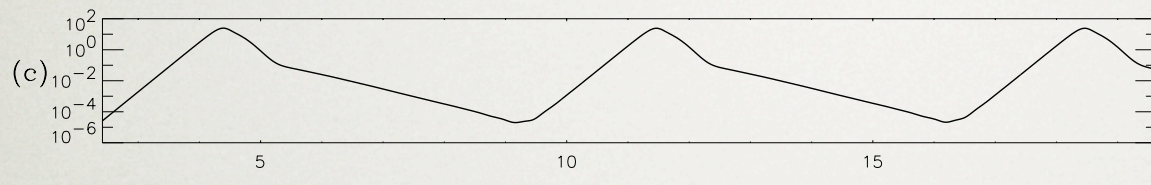
$$\hat{B}_{\bar{x}}(\bar{y}, t) = e^{-\sigma t} \langle B_{\bar{x}} \rangle_{\bar{x}, z}$$



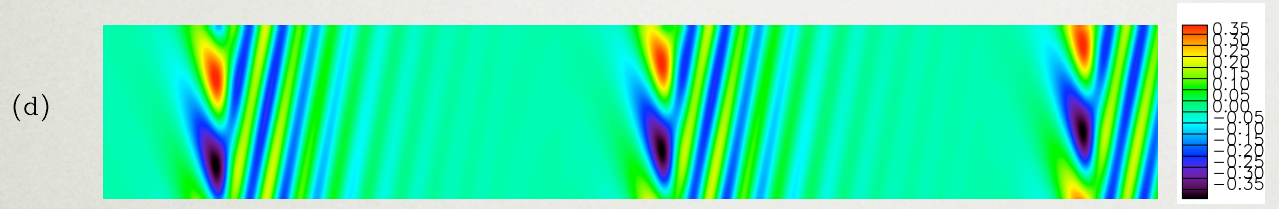
$E_K$



Rolls

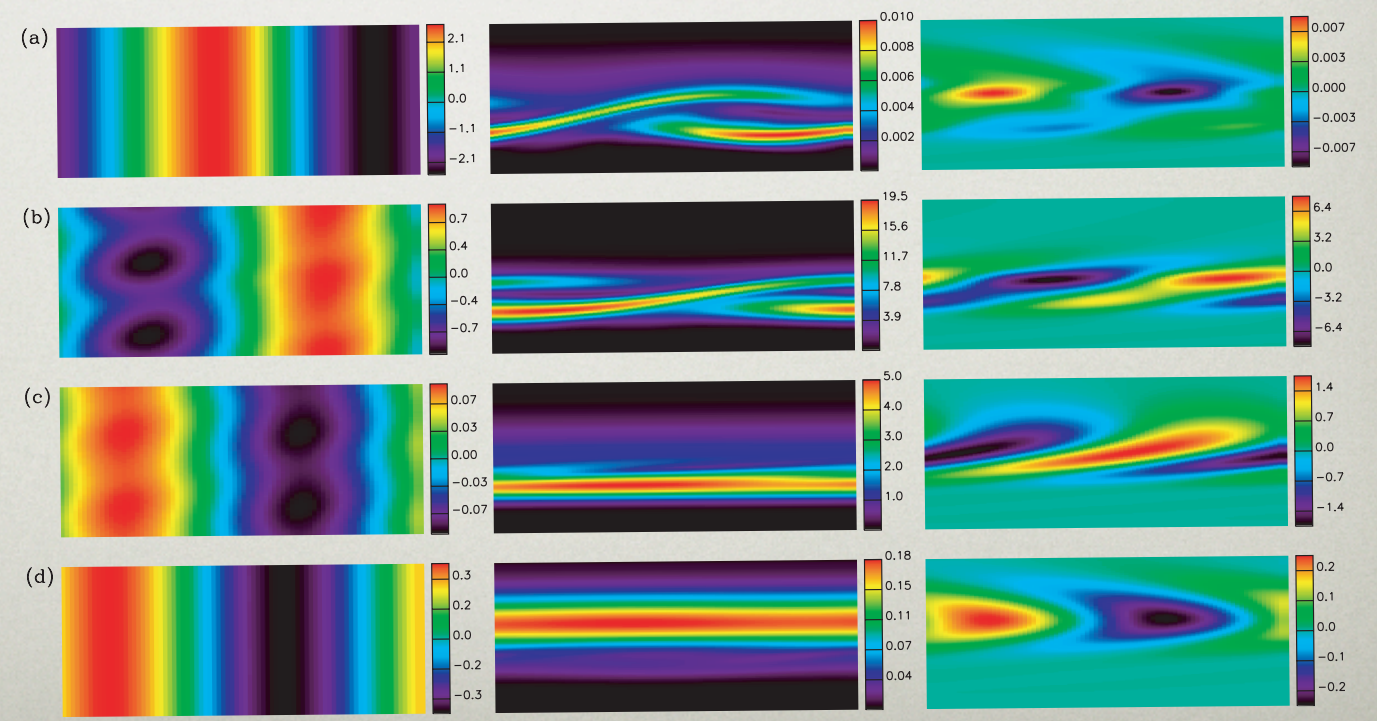


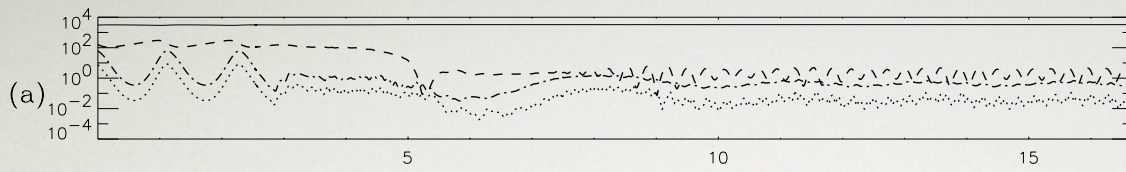
$E_M$



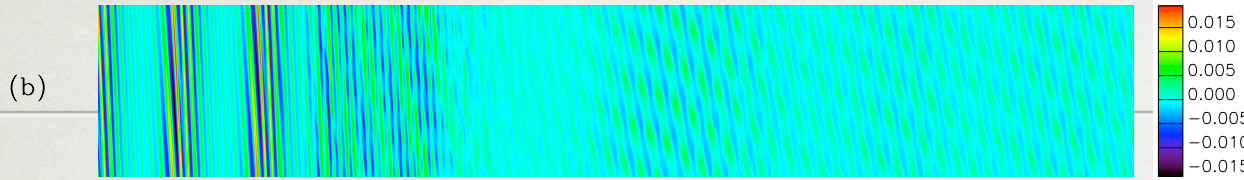
B-field

Dynamical  
behaviour at  
 $Re=210, Pm=50$   
 $Pmc=9$

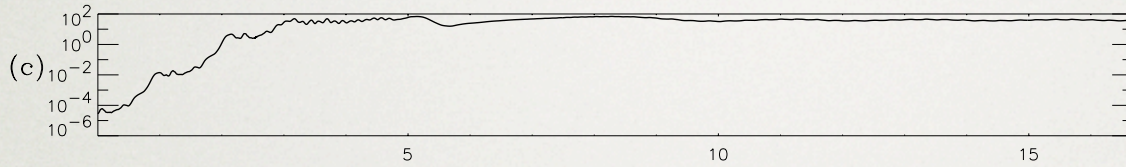




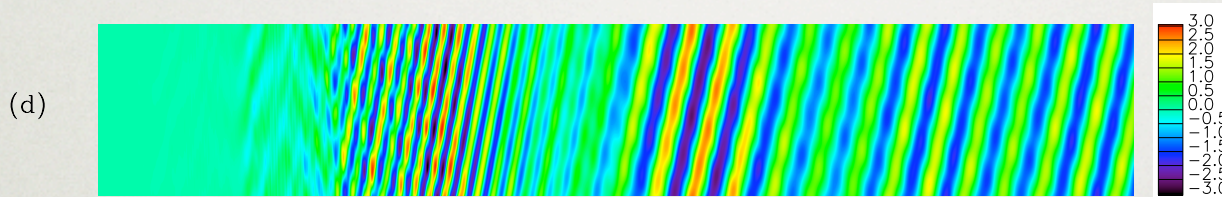
$E_K$



Rolls



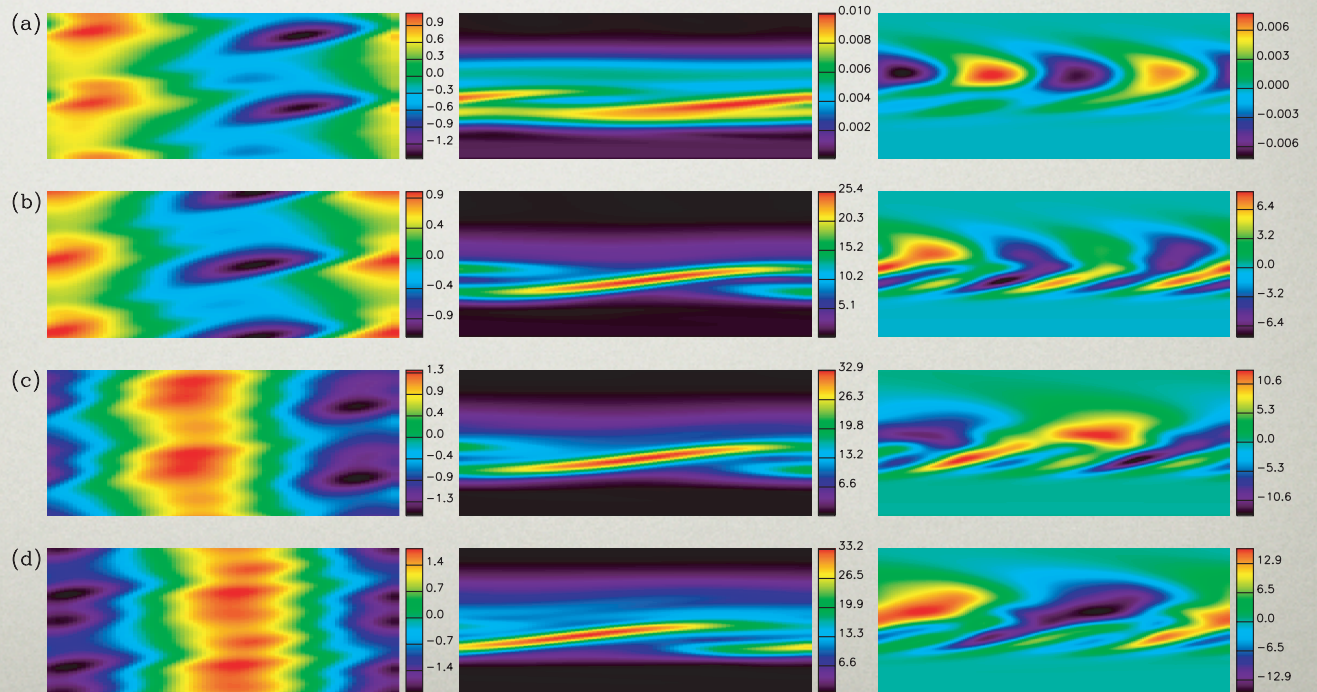
$E_M$



B-field

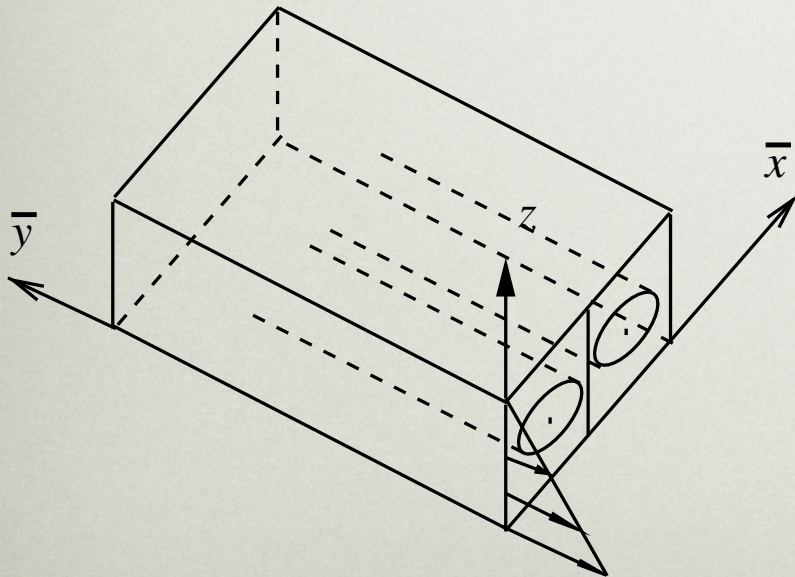
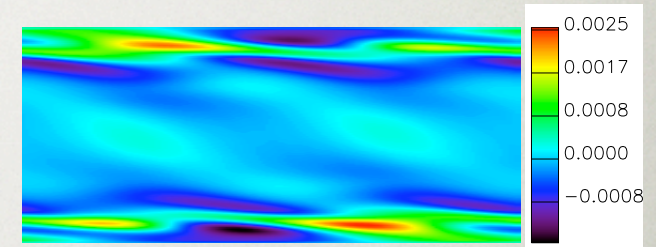
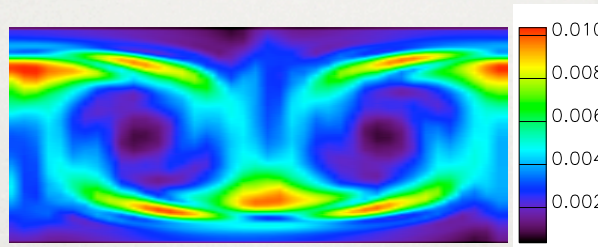
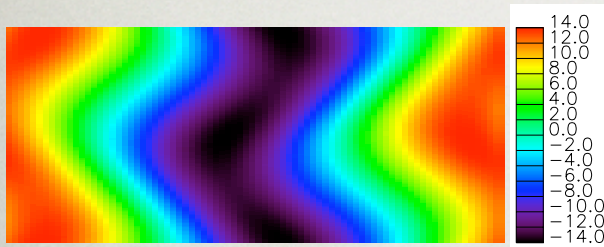
Dynamical  
behaviour at  
 $Re=250, Pm=50$

$Pmc=28$



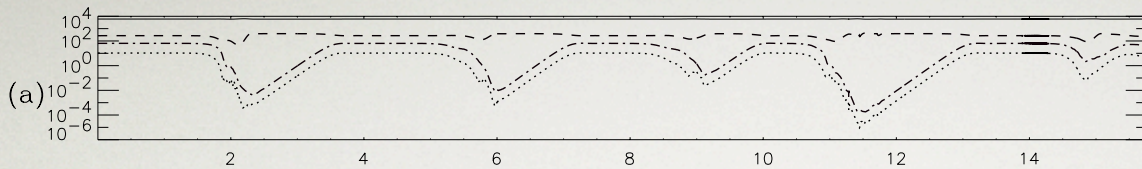
# WAVY TAYLOR COUETTE: KINEMATIC DYNAMAMO

$$\tau = 22, \quad \text{Re} = 200, \quad \vartheta = 90^\circ, \quad \varepsilon = 90^\circ, \quad k_{\bar{x}} = 3.117, \quad k_{\bar{y}} = 1.$$

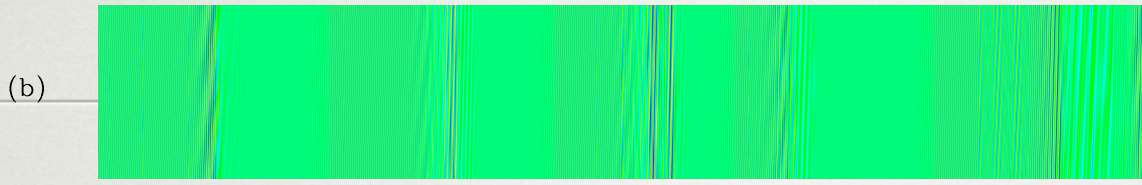


Bifurcation to steady  
wavy rolls at  $\text{Re}=190$

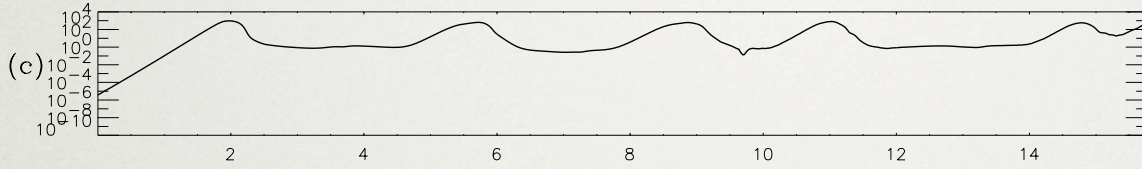
$$\text{Pmc}=13$$



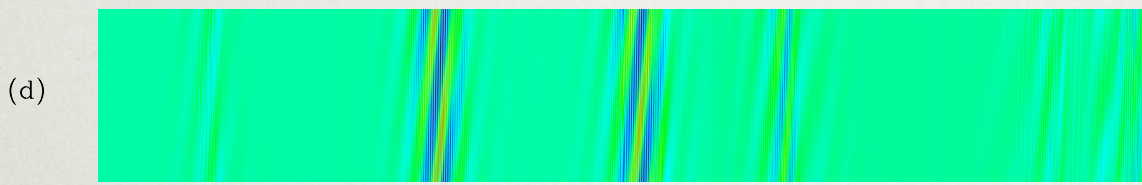
$E_K$



Rolls



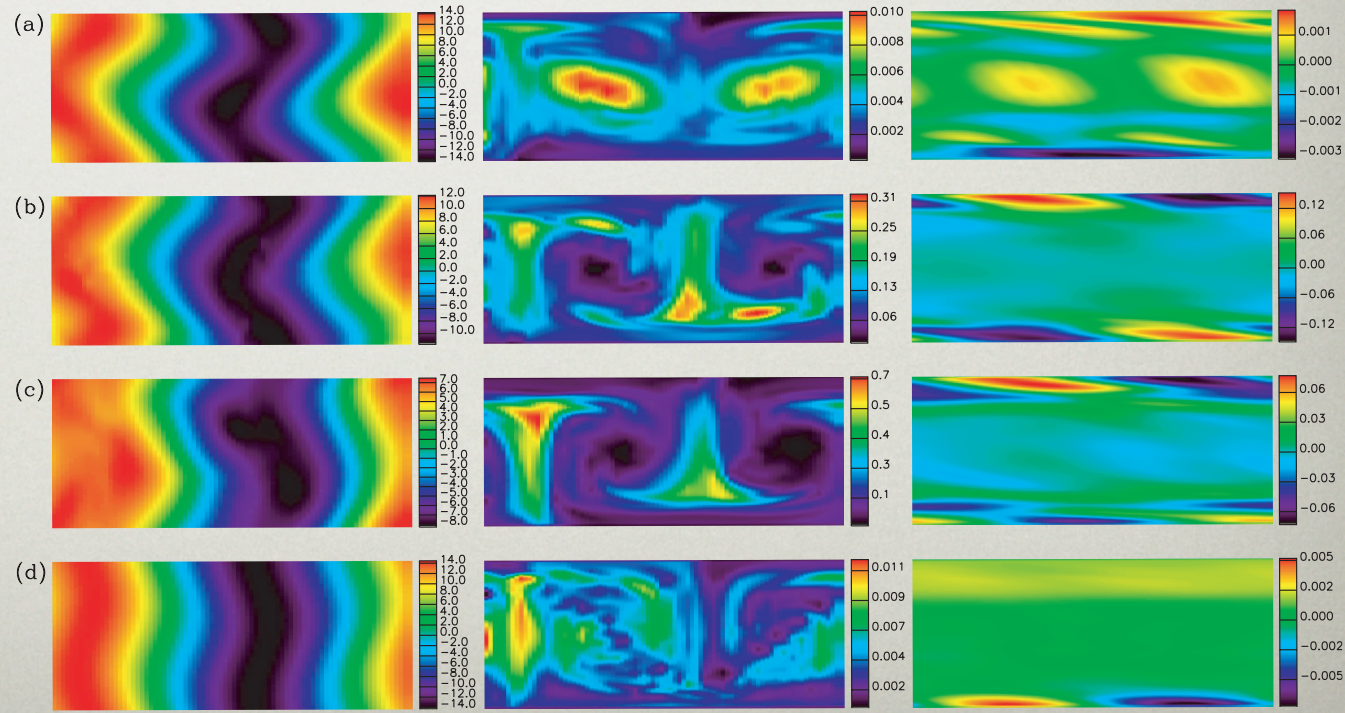
$E_M$



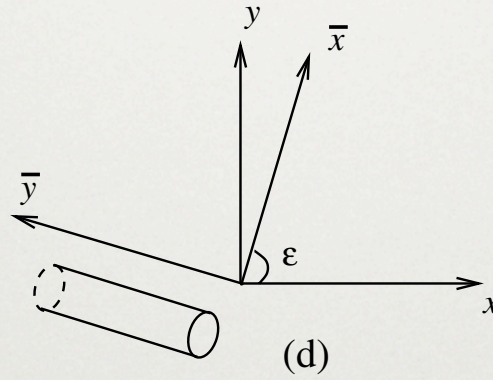
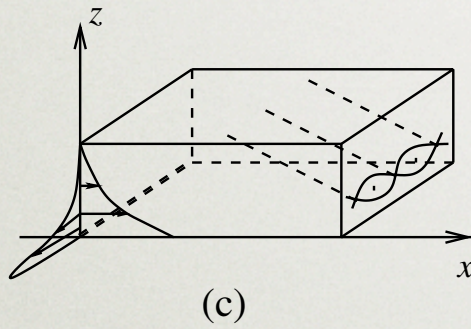
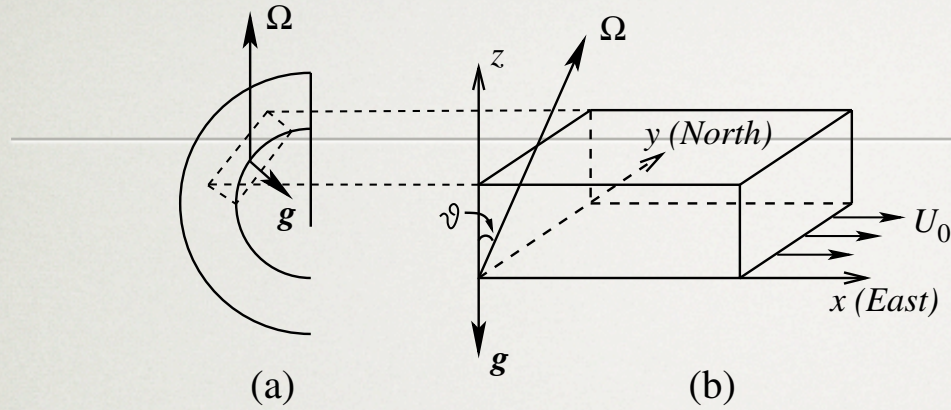
B-field

Dynamical  
behaviour at  
 $Re=200, Pm=50$

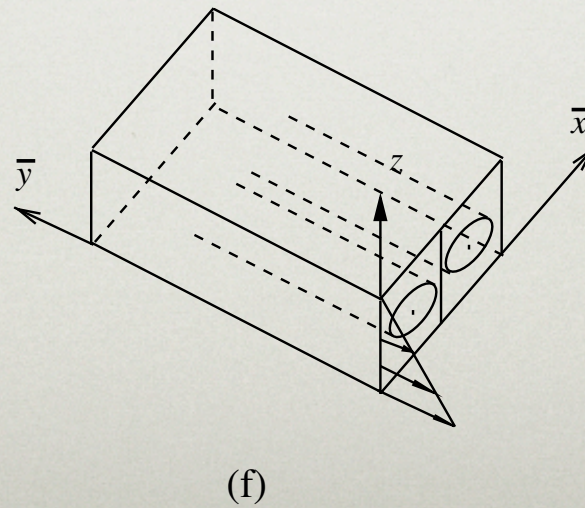
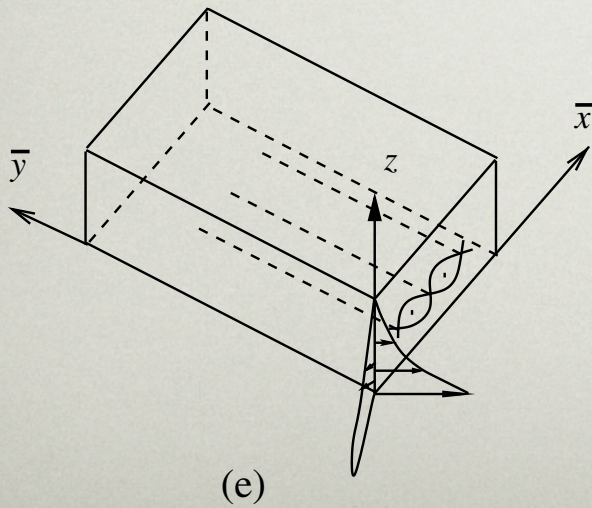
$Pmc=13$



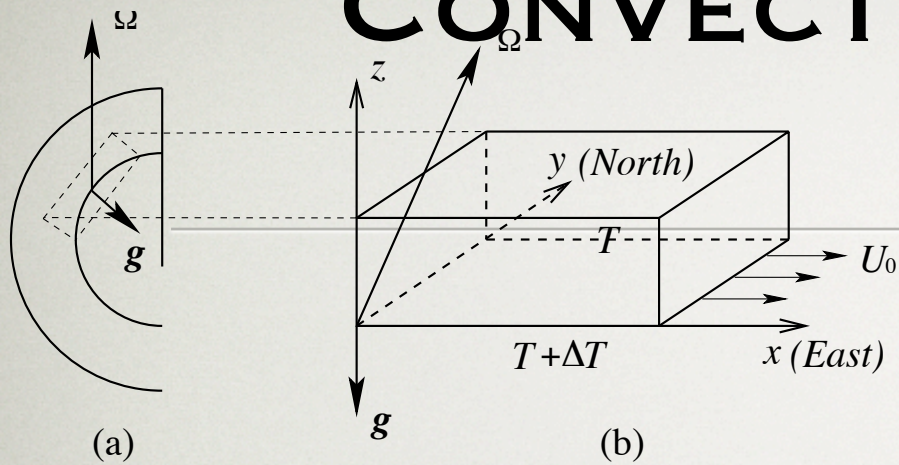
# GEOMETRY



Note cat's eyes or TC rolls have axes approximately aligned with the shear.



# CONVECTIVE EXAMPLE



Convective roll axes here aligned with horizontal component of rotation.

$$Ra = 7500 \simeq 2 Ra_c, \quad Re = 30, \quad \tau = 200,$$

$$P = 1, \quad q = 50, \quad \vartheta = 67.5^\circ, \quad k_x = 4.30, \quad k_y = 1.0,$$

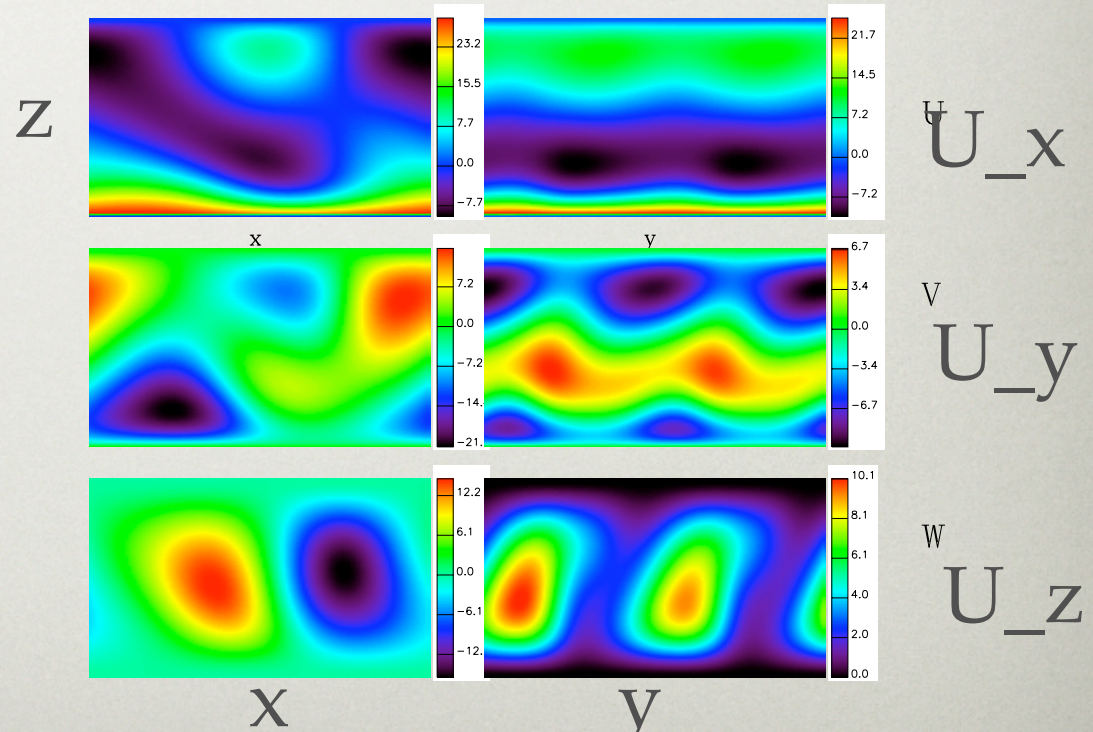
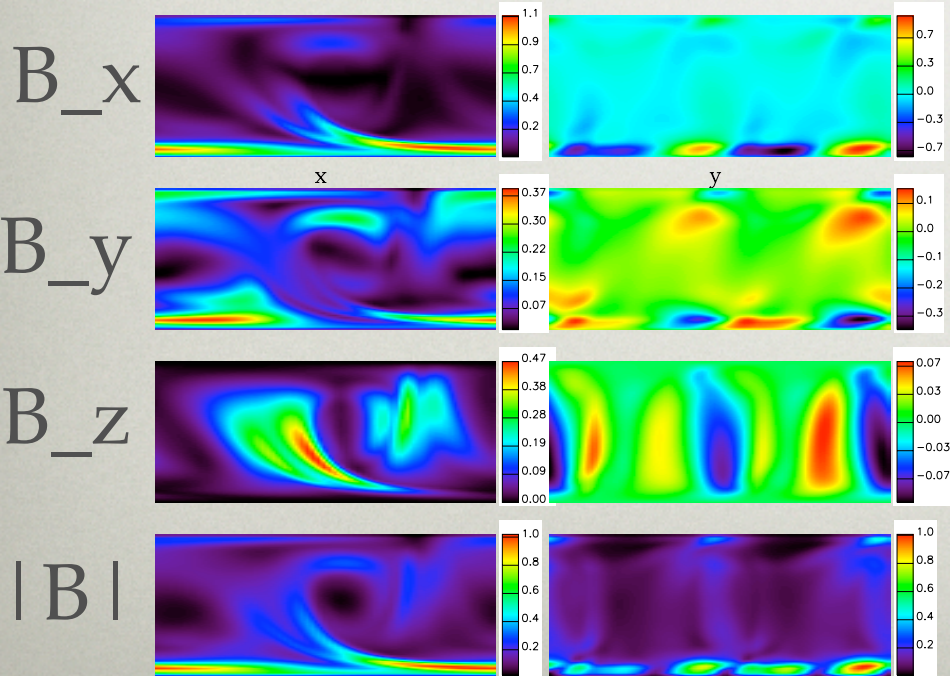
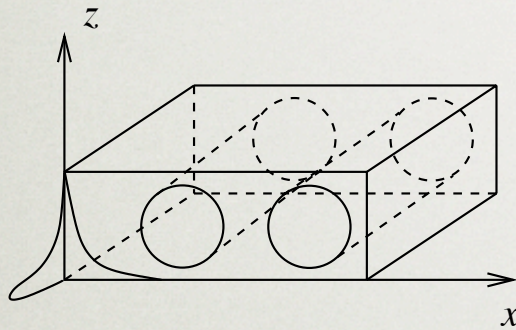
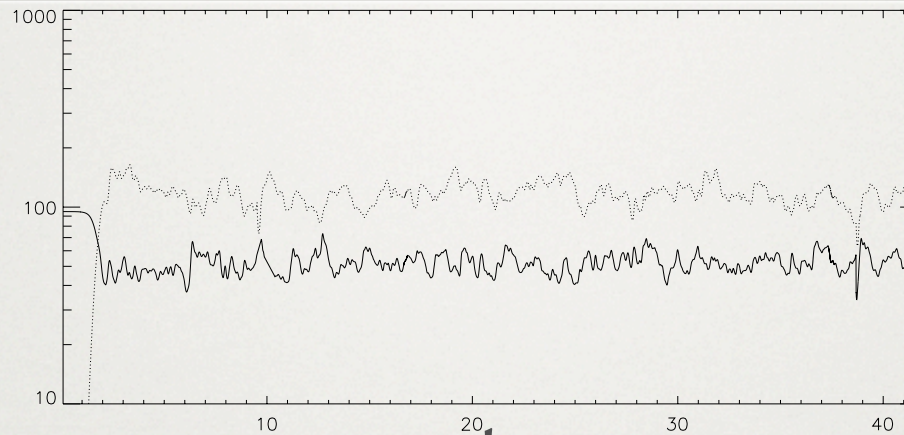


Fig. 2. Convective flow in the kinematic regime, with parameter values (3.1), (3.2). Plotted are the flow components ( $U, V, W$ ) of  $\mathbf{U}$  in the  $(x, z)$ -plane (left-hand panels) and  $(y, z)$ -plane (right-hand panels).

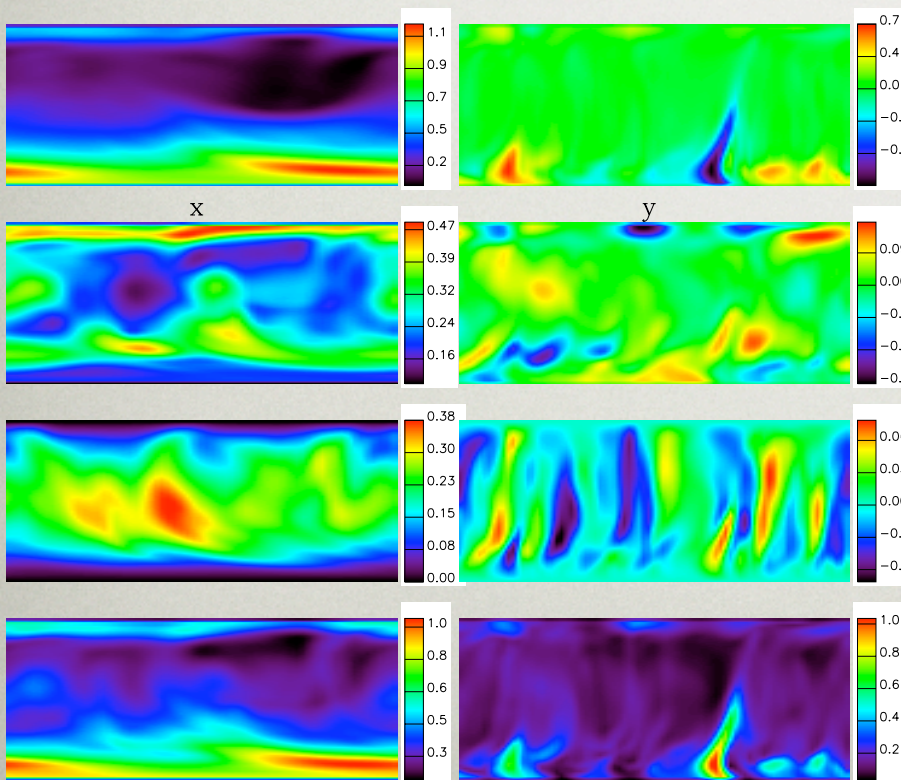
# DYNAMICAL REGIME

E\_K, E\_M

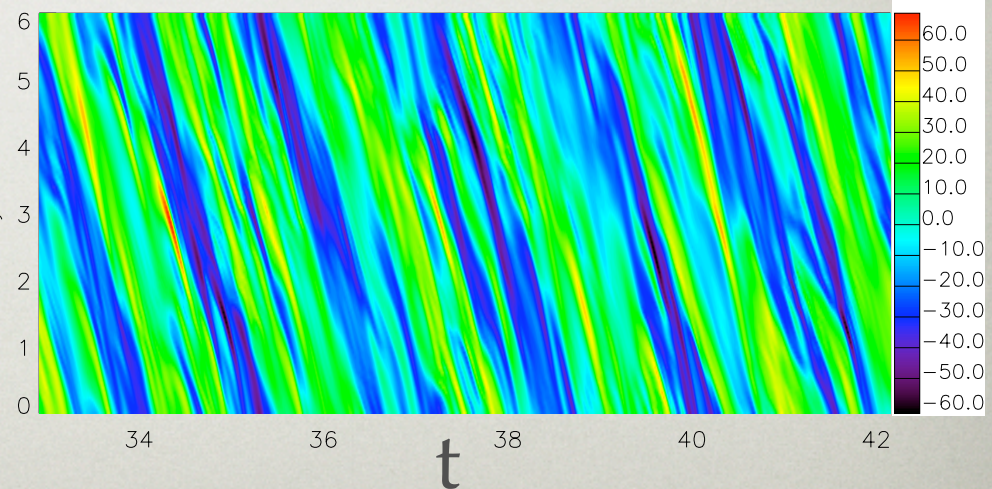


t

Alpha-omega dynamo:  
waves and phases



y



$$\hat{B}_x(y, t) = \langle B_x(x, y, z_{\max}, t) \rangle_x$$

# CONCLUSIONS

- Ekman instabilities and T-C support dynamos,

---

- complex, relatively incoherent field structure,
- weak magnetic energy, similar to perturbation  $E_K$ ,
- relaxation oscillations common: magnetic field tends to turn off the shear instability,
- convective 'interface' dynamos give coherent, strong fields ( $E_M \sim E_K$ ) and alpha-omega waves,
- convective dynamos more likely in solar context, also in view of stratification,
- limitation: only moderately supercritical.